FRACTURE TOUGHNESS BEHAVIOUR OF FRPs REINFORCED BY ALUMINIUM PARTICLES AT THE INTERFACES

by

ANIL R. GAWAHALE

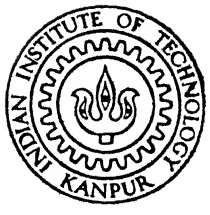

DEPARTMENT OF MECHANICAL ENGINEERING
INDIAN INSTITUTE OF TECHNOLOGY KANPUR

MARCH, 1990

FRACTURE TOUGHNESS BEHAVIOUR OF FRPs REINFORCED BY ALUMINIUM PARTICLES AT THE INTERFACES

A Thesis Submitted
in Partial Fulfilment of the Requirements
for the Degree of

MASTER OF TECHNOLOGY

by

ANIL. R. GAWAHALE

to the
DEPARTMENT OF MECHANICAL ENGINEERING

INDIAN INSTITUTE OF TECHNOLOGY, KANPUR

MARCH, 1990

CERTIFICATE

This is to certify that the thesis entitled "Fracture Toughness Behaviour of FRPs Reinforced by Aluminium Particles at the Interfaces", by Anil R. Gawahale is a record of work carried out under my supervision and has not been submitted elsewhere for a degree.

Dr. Prashant Kumar
Professor
Dept. of Mech. Engg.
I.I.T. Kanpur

March, 1990

ABSTRACT

Effect of reinforcing the interfaces by aluminium particles was studied on two kinds of laminates, glass fabric reinforced epoxy and carbon fibre reinforced epoxy. Fracture toughness tests under mode II were conducted on precracked ENF specimens. The increase in fracture toughness value of glass fabric reinforced epoxy specimens with aluminium particles sprayed at the interfaces was observed in case of 15°, 3Ø° and 45°; whereas Ø° specimens, which does not form an interface, showed decrease in fracture toughness value G_{IIc}. The reduction in tensile strength and modulus was observed. For CFRP laminates, mixed behaviour was observed as the ply angle was varied. Micrographs showed that the aluminium particles caused the bowing of the fibres in the glass fabric reinforced epoxy laminates.

Dedicated

To

My Parents

ACKNOWLEDGMENT

I praise God Almighty for his persistent grace.

I owe debts of gratitude and respect to my thesis supervisor, Dr. Prashant Kumar for his expert guidance, constant encouragement and pleasant interaction.

My rendering to Dr. B.D. Agarwal, Dr. P.K. Singh, Mr. Basant Goel, for their friendly rendering of all possible support and the valuable discussions I had with them.

Let me compliment the staff of E.S.A. Lab, Manufacturing Science, ACMS, for their immense help.

It is with pleasure that I recall my association with all my friends who helped me during various stages.

Last but not the least, a word of praise for Mr. Suidhir for his typing.

Anil R. Gawahale

CONTENTS

LIST OF FIGURES

LIST OF TABLES

NOMENCLATURE

G	energy release rate
G_{II}	mode II interlaminar fracture toughness
H	potential energy
U	elastic strain energy stored in the body
W	work supplied by the external forces
A	crack area
p	load on the fracture toughness testing specimen
Pc	critical load on the fracture toughness testing specimen
u	load point displacement
C	compliance of the specimen
G_{IIc}	critical mode II interlaminar fracture toughness
E_I	flexural rigidity
a	starter crack length in the specimen
w	width of the specimen
h	semi thickness of the ENF specimen
l	half span in ENF testing
A_{proj}	projection of actual fractured area

CHAPTER 1

INTRODUCTION

1.1 INTRODUCTION

Upto about two decades ago the main structural materials used were metals like aluminium, titanium, steel etc. As the requirements on materials grew specially on high strength, high stiffness, light weight, and less prone to corrosion, a new class of materials fibre composites, began to develop rapidly. Composite materials in some form or the other have existed for many years but fibre reinforced composite materials are found useful only after high strength man made fibres of glass, carbon, kevlar have been developed .

Composites differ from conventional engineering materials, because a second material phase is added to a matrix to obtain specific performance characteristics not available from the unmodified materials .The second phase is generally added to provide strength, stiffness and light weight .

Fibre composites are usually made from plies or laminae; in each ply fibres are either in unidirectional or in woven form. One of the most common way is to make the laminate from prepregs. A prepreg is a cloth made from fibres embedded with the resin which is in a semicured state also termed as B-staged. At room temperature ,the prepregs can be worked on easily ;i.e ,it can be cut like a tailor cuts the patterns and then can be stacked as desired . The stack is then pressurized and heated through a recommended cycle to obtain the final laminate .

Some of the teething problems faced by these high potential fibre composites are high cost of fibres and resins and the manufacturing of the laminae. Also unlike metals the laminates are susceptible to delamination under adverse service conditions.

Composite materials are observed to fail by (i) breaking of the fibres, (ii) Cracking of the matrix, (iii) separation of fibres from the matrix (called debonding) and (iv) delamination (separation of the interface of two adjacent laminae with different fibre orientations). These modes may act separately or jointly [1].

Out of these failure modes , the delamination has been found to be one of the major reason for the failure of laminated composites under impact . The susceptibility to delamination is more because :

(i) there is no through the thickness reinforcement of high strength fibres .

(ii) stress discontinuity is observed between the two plies with different fibre orientations due to difference in effective modulii and

(iii) the interlaminar (delamination) cracks easily propagate because the region between two plies is epoxy rich which is generally brittle.

Thus the laminates are less tough and fracture cracks spreads easily to long distances. Furthermore, the damage can spread in the interfaces deep inside the thickness and may not be detected easily. Delamination growth redistributes the stresses

in the plies of a laminate, and may influence residual stiffness, residual strength and fatigue life. These lead to the loss of structural integrity and contribute to the final failure of the structure. Therefore to make the composite components durable it is important to increase the interlaminar toughness for structural components.

1.2 DELAMINATION TOUGHNESS

In order to understand the interlaminar toughness, let us briefly review the basic principles of the fracture mechanics. In fracture mechanics two basic approaches have emerged, namely the energy and the stress approach. The first approach is due to Griffith [2] who on the basis of thermodynamic considerations derived a criteria for fracture, by taking account of the total energy change in a cracked body. The second approach is due to Irwin [3] who relied on the stress field in front of a crack tip. The stress field is characterized by a parameter, stress intensity factor K.

The stress analysis ahead of a crack tip in a composite material is an extremely difficult problem because of the local heterogeneity and anisotropy. Thus, it has become a common practice to characterize interlaminar fracture with the energy release rate G. In fact, when a crack propagates two new surfaces are formed. Energy should be supplied by the system to form the new surfaces. Thus, G is the energy release rate per unit area of crack extension. This brings in the concept of critical energy release rate G_C. If the system is capable of releasing energy more than G_C, then only the crack will propagate. G is

mathematically well defined as well as physically measurable in experiments. In the application of the energy principle it is not necessary to specify the constitutive properties of the system; also the body may be isotropic or anisotropic, linear or nonlinear.

Another approach through J-integral is used very commonly to characterize crack propagation in metals. J-integral is also an energy approach but is capable of dealing complex cases of inelasticity such as plastic flow infront of a crack tip. However, in the case of composites specially made from epoxy as matrix material, the crack propagates with a very small plastic zone infront of the crack tip and for all practical purposes, the interlaminar crack propagation can be considered as elastic, then J reduces to G.

A crack propagation in general, may occur by three modes designated as mode I, mode II and mode III (Fig. 1.1). In mode I, failure is produced by a tensile stress applied at right angle to the laminate plane, resulting in opening up of the laminate (opening mode); in mode II, failure is caused by an in-plane shear stress (forward shear mode); in mode III failure is by antiplane shear stress (parallel shear mode).

A delamination crack propagates only between two plies and may be likely to occur any one of the three modes. However, in most of the practical cases, stresses due to bending moment or and transverse loads are generated. The bending moment do generate tensile stresses but they act parallel to plane of the laminate faces and therefore cannot have the delamination crack

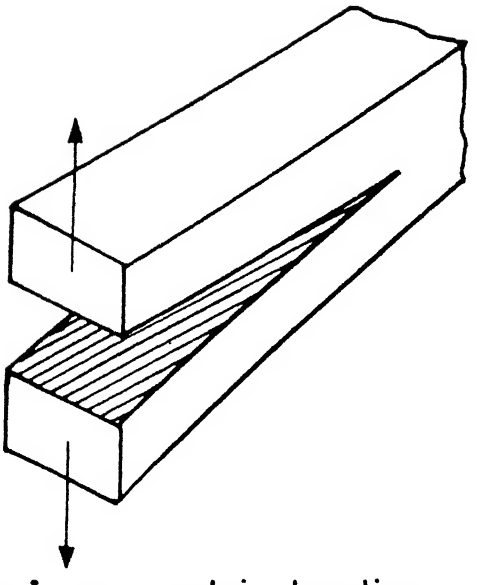

(a) Mode I: symmetric loading
(opening mode)

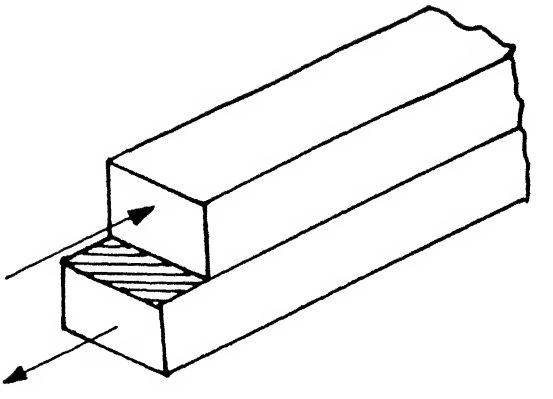

(b) Mode II : skew symmetric
shear loading
(forward shear mode)

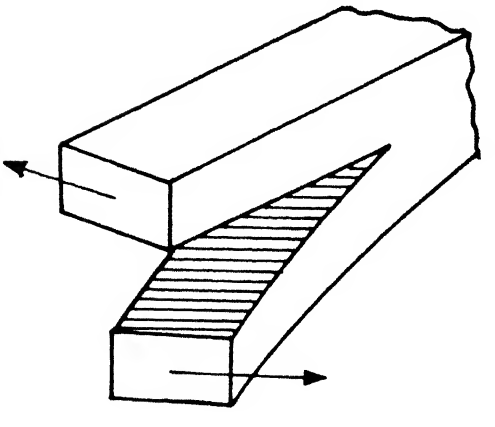

(c) Mode III : antiplane shear loading
(parallel shear mode)

Fig.1.1 Modes of crack surface displacement.

propagation in mode I. On the other hand, transverse load develops shear stresses which apply loads on the delamination crack in mode II. Therefore a laminate is mainly susceptible to delamination crack growth in mode II.

1.3 ENHANCEMENT OF INTERLAMINAR FRACTURE TOUGHNESS

Various studies have shown that braiding, 3-D, 2.5-D weaving and through the thickness stitching offer promise for improved damage tolerance, interlaminar fracture toughness and capability to withstand out of plane loads. However, fabrication of laminates through such techniques is still in the early stages of developments [4].

A.C. Garg [5] have demonstrated that presently used thermosets (epoxies) may be toughened by adding thermoplastics. Thin discrete layers of a tough ductile resin are interleafed at the lamina interface. This increases the impact damage tolerance, compressive strength and residual strength but it reduces tensile strength, young's modulus (E).

In another approach whiskers have been mixed in epoxy before wetting the fibres. These whiskers reinforce the epoxy rich interface and enhances the delamination toughness. However, the tensile strength reduces considerably [6].

In the present work, to enhance the G_{IIc}, aluminium particles on glass fabric rich epoxy prepregs were sprayed before they were stacked and hot pressed. The particles reinforce the epoxy rich areas but unlike the work on whiskers [6], they do not weaken the interior of a laminae.

1.4 DETERMINATION OF G_{IIc}

A convenient test technique is needed to determine the critical energy release rate G_{IIc}. In 1985, Russel and Street [7] put forward a method to measure mode II interlaminar fracture toughness of unidirectional composites with end notched flexure specimen (ENF). In 1986, Carlson [8] made a detailed discussion on ENF method, including specimen size, stability of crack growth and influence of friction between crack surfaces. T. Vu Khanh [9] discussed the conditions for pure mode II measurements and recommended that the starter crack should be introduced at the mid plane of the specimen. James M. Whitney [10] have used centre notched flexure (CNF) specimen for mode II under impact loading. The ENF specimen have been used by G. Moron et al. [11] to determine mode II fracture toughness for various types of fibre reinforcements.

1.5 OUTLINE OF THE PRESENT WORK

In the present work, matrix rich interfaces of glass fabric-epoxy laminates were reinforced by aluminium particles of the size approximately equal to the diameter of the fibres. The critical energy release rate G_{IIc} was determined statically through the ENF method.

The delaminated surfaces were observed under the electron scanning microscope to study the particle distribution and delaminated region.

In chapter 2, the details of specimen preparation are discussed. Chapter 3 gives the theoretical and experimental

aspects of the mode II interlaminar fracture toughness determination. The results of the work and discussion are given in chapter 4. Chapter 5 concludes the present work.

CHAPTER 2

SPECIMEN PREPARATION

2.1 INTRODUCTION

Specimens were prepared to test the interlaminar fracture toughness in mode II through the End Notched Flexure (ENF) test described in detail in chapter 3.

Laminates were made from glass fabric epoxy prepregs and from carbon fabric reinforced with epoxy. A prepregs is a thin sheet made from fibres embedded in a resin which is in semicured state(B-staged). At room temperature, the prepregs can be easily worked on, i.e. can be cut like a tailor cuts the patterns and the cut specimens can be stacked over as described. The stack then has to go through heat-pressure cycle recommended by the supplier of the prepregs to obtain the final laminate.

2.2 FABRICATION OF GLASS FABRIC REINFORCED EPOXY LAMINATES

Glass fabric reinforced epoxy laminates were made from prepregs, bought from Tech-Invest(India) Pvt. Ltd., BHEL Industrial Estate, Hardware, UP, with the following specifications supplied by the company :

TYPE	: Glass Fabric / Epoxy (Rich)
REINFORCEMENT	: Glass fabric finely woven, approximately balanced (36 x 32 counts per 25mm) with area density of 185 gm/sqm.
MATRIX	: Epoxy LY 556 with Hardener HT 976 and HT 973 mixed in the ratio of 100:35:1 respectively
WIDTH OF PREPREG	: 1 meter

The prepreg was cut into small pieces of the size 125x125 mm. Twentynine layers were stacked over each other according to the desired orientation. Some preparations are needed before the stack is hot pressed, which are (Fig.2.1) :

(i) On each side of the stack Uniphane BOPP (biaxially oriented polypropylene) release film is provided. The films has punched holes of 1.2mm diameter with interhole distance of 1Ø mm to bleed out the extra epoxy from the top and the bottom surfaces.

(ii) The 5 mm thick felt was placed on either side of releasing film to absorb the extra epoxy which bleeds out through holes in the release films.

(iii) Aluminium retaining plate of 1.5 mm thick with a square hole of 155 mm and teflon spacer blocks of 1Øx1Øx6 mm size placed between the plies and internal edges of the square hole to keep the plies in place during hot pressing.

(iv) The teflon sheet was provided at the back of each felt so that the absorbed epoxy in felt does not stick to the platens of the press.

This assembly is placed between the two platens of a press as shown in Fig.2.2 and Fig.2.3. In the upper and lower platens of the press, the heating elements are already built in ; the heaters are thermostatically controlled. For application of pressure, a hydraulic jack of 2Ø ton capacity along with pump assembly was used. The temperature of the laminate is measured with the copper-constantan thermocouple. Its end is embedded in the composite plate and generated voltage is measured through a digital milli-voltmetre.

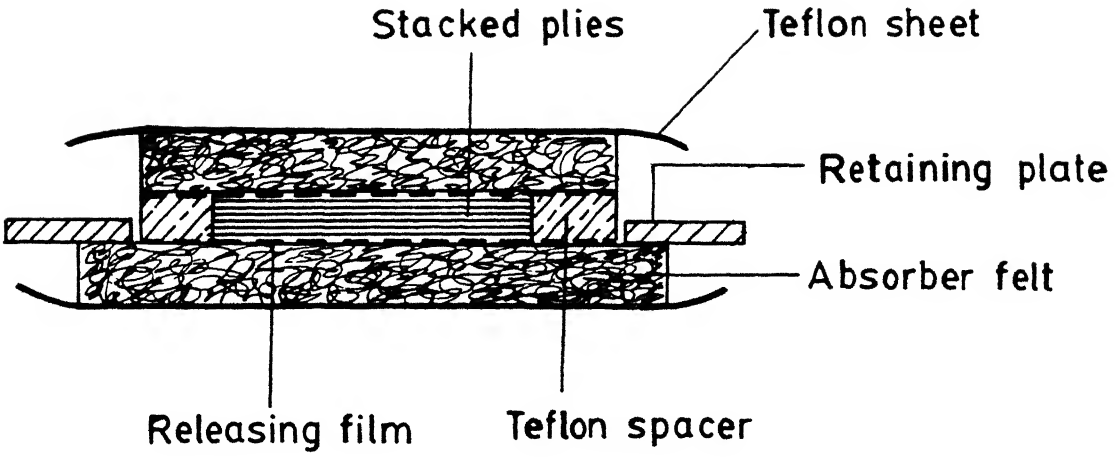

FIG. 2·1 CROSS SECTIONAL VIEW OF STACKED PLIES ASSEMBLY

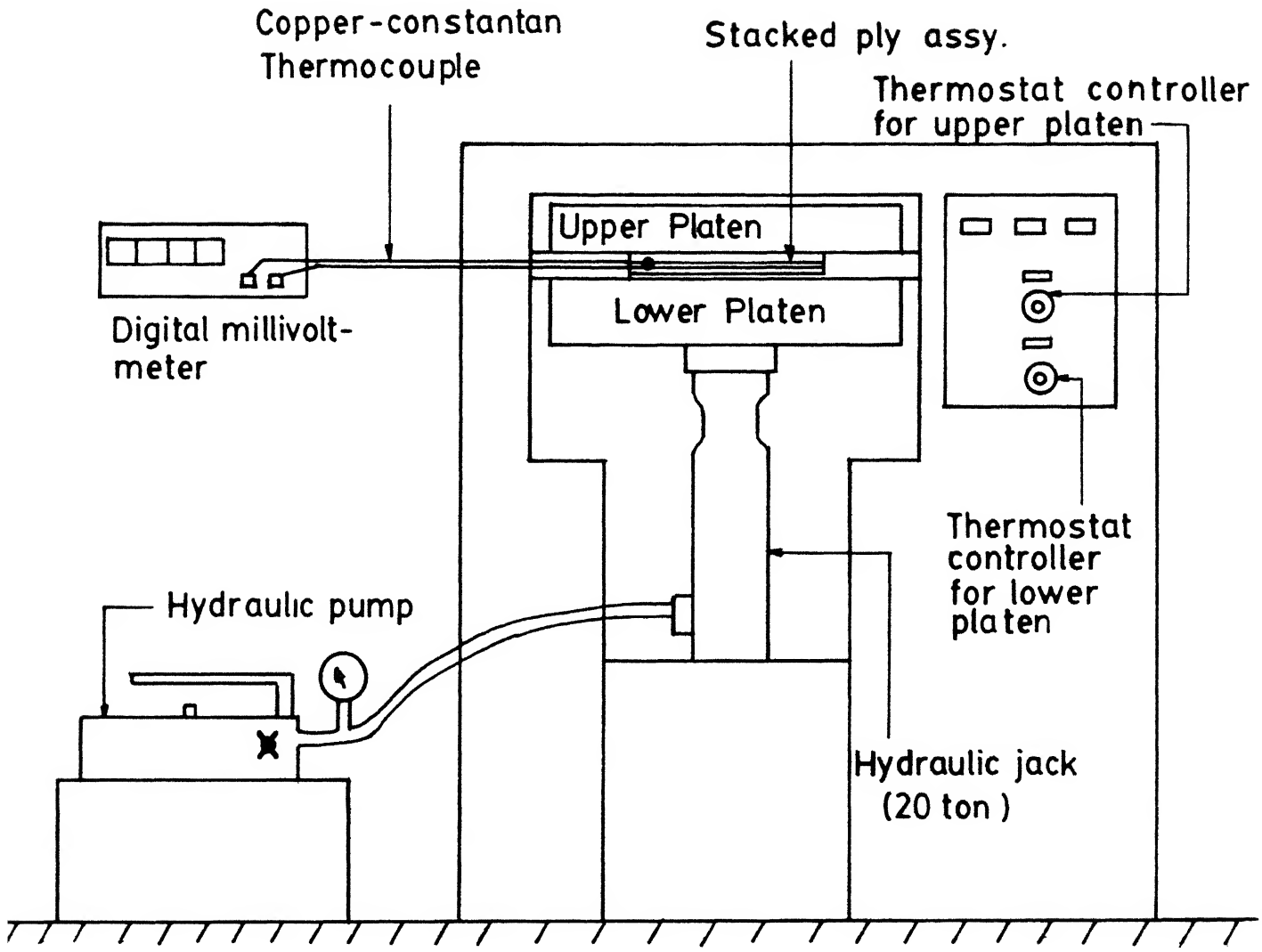

FIG. 2.2 SCHEMATIC VIEW OF THE PRESS

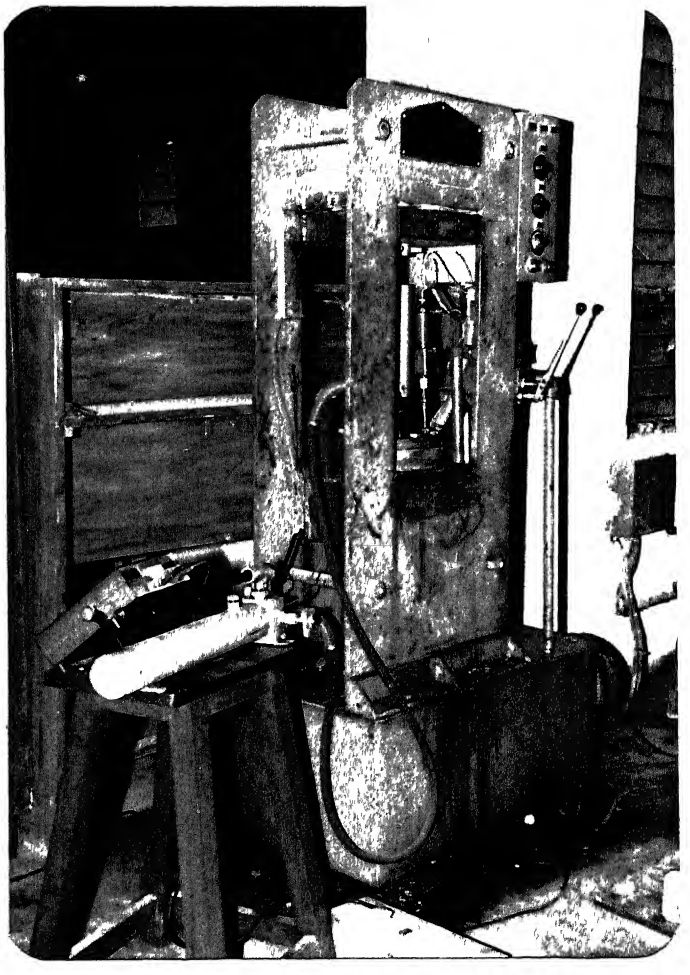

Fig.2.3 Hot-press view applying heat and pressure

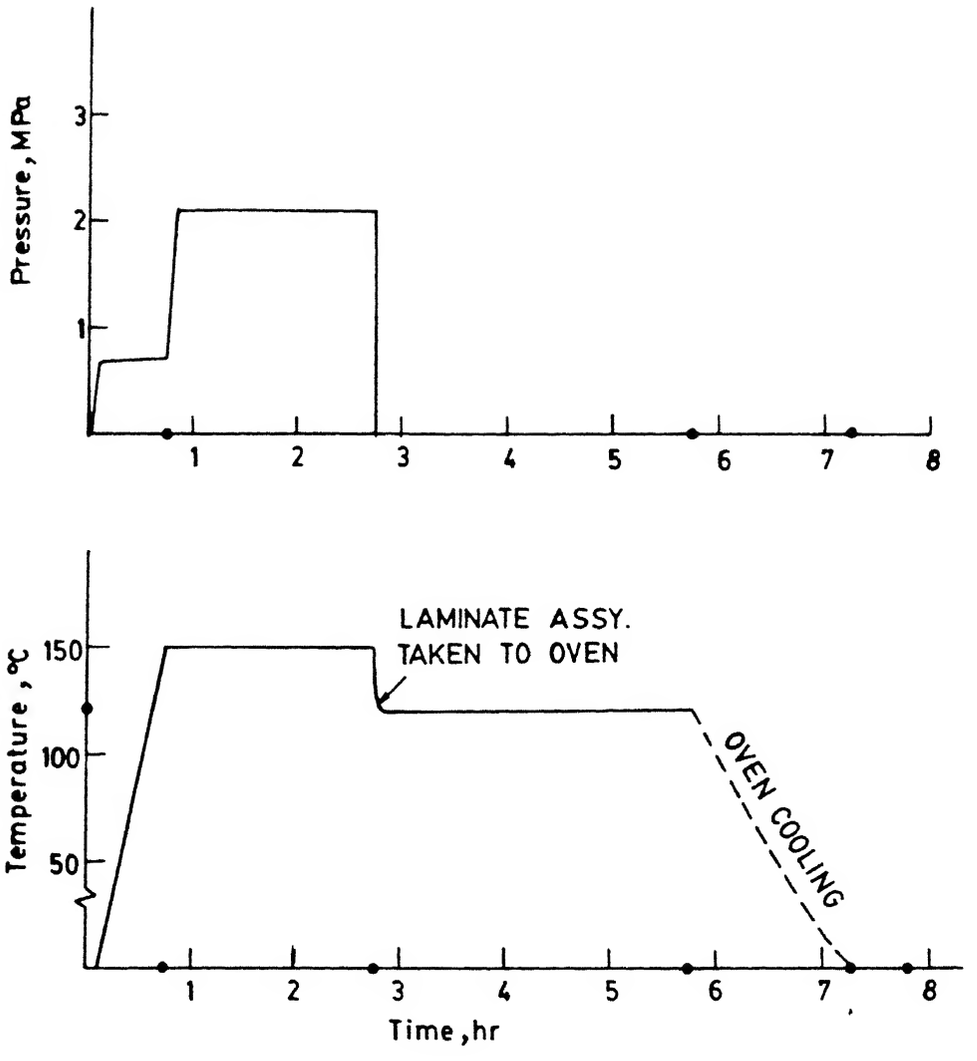

FIG. 2·4 HEAT AND PRESSURE CYCLE FOR LAMINATE CURING

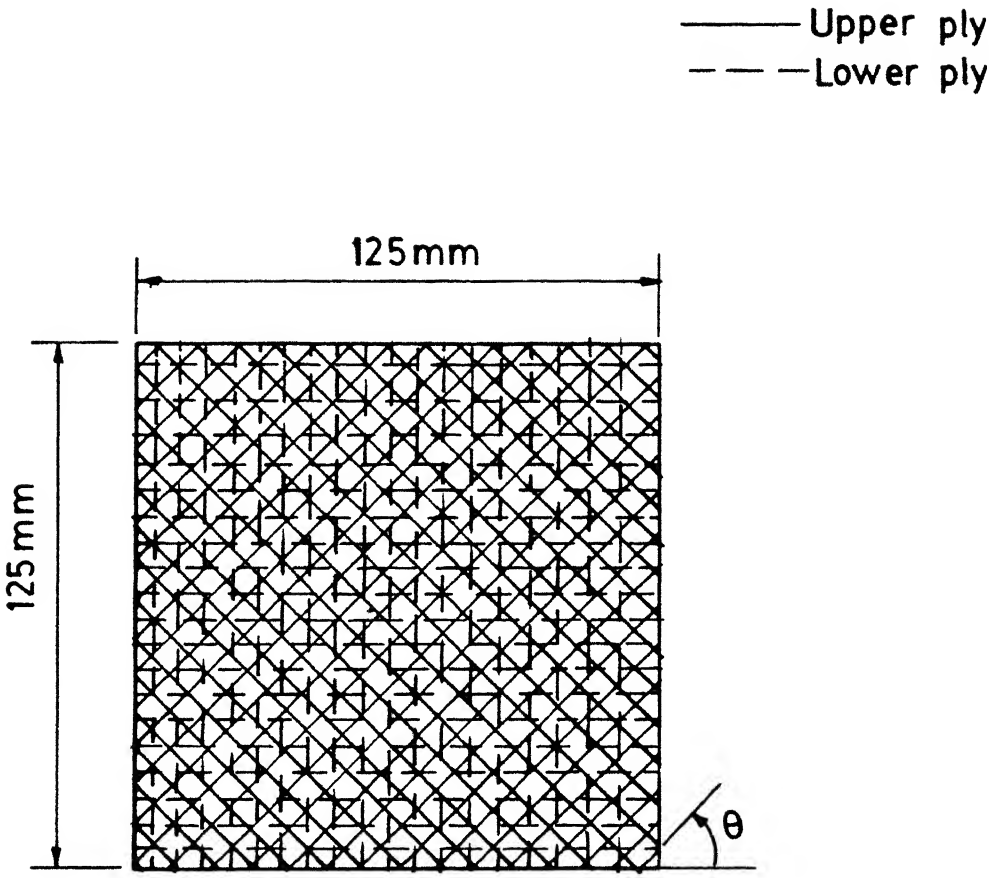

FIG. 2·5 ORIENTATION OF NEIGHBOURING PLIES OF GLASS FABRIC

The assembly was placed in the press at room temperature with an initial pressure of 70 x 10^{-2} MPa. The heaters were switched on and the temperature was allowed to reach 150°C. When it attained the temperature of 150°C the pressure was increased to 205 x 10^{-2} MPa. The temperature and pressure were maintained for two hours as shown in Fig. 2.4. Afterwards, the pressure was released and the laminate assembly was taken out of the press and post cured in an oven for three hours at 120°C. It was then allowed to cool down to room temperature in the oven which takes about one and half hour.

The laminate was separated out from release films, felt, teflon sheets etc. and the laminate was checked visually for voids and air entrapment. The colour was dull green with translucent appearance. One could see the shape of the fingers placed behind the laminate.

Four kinds of laminates were fabricated based on angle between the neighbouring plies Fig. 2.5. They are :

(i) $[(0/90)_6 / 0 / 90 / \bar{0}]_s$

(ii) $[(0/15)_6 / 0 / 15 / \bar{0}]_s$

(iii) $[(0/30)_6 / 0 / 30 / \bar{0}]_s$

(iv) $[(0/45)_6 / 0 / 45 / \bar{0}]_s$

2.3 FABRICATION OF CARBON FIBRE REINFORCED EPOXY LAMINATES

Carbon fabric reinforced epoxy laminates were made from unidirectional weave of Carbon fabrics G 808 with warp and weft in ratio of 91 : 9. The epoxy was made from Resin LY 556 and Hardener HT 1907 IN with accelerator DY 062 in the ratio of 100 : 85 : 1.5 respectively. The pot life of the epoxy is 24 Hrs,

because jel formation of epoxy does not take place while using it The unidirectional carbon fabric were cut by the size 22Ø x 22Ø mm. On each layer the epoxy is applied with the help of brush. Nineteen layers were stacked over each other according to the desired orientation. On each side BOPP (Biaxially Oriented Poly Propylene) release film is provided, behind the release film a mylar sheet (174 μm thick) and a woolen felt of 6 mm thickness is provided respectively. Along the edges of laminate the felt strips are provided so that extra epoxy does not readily flow out. The assembly is placed between the two aluminium plates to be hot pressed between two platens of the press. The initial pressure of 3 KPa is applied till the temperature of 12Ø°C is reached ; at this temperature the jel formation starts to occur and the pressure is increased to 9 KPa. This temperature and pressure is maintained for half an hour. Afterwards, the pressure was released and the laminate assembly is taken out of the press and post cured in an oven for three hours at 8Ø°C. It was then allowed to cool down to room temperature in the oven which takes about one hour.

The laminate was separated out of the release films, and was ready for specimen preparation.

Four kinds of laminates were fabricated, each having six interfaces with the following orientations :

(i) $[Ø_3 / 9Ø_3 / Ø_3 / \overline{9Ø}]_S$

(ii) $[Ø_3 / 3Ø_3 / Ø_3 / \overline{3Ø}]_S$

(iii) $[Ø_3 / 45_3 / Ø_3 / \overline{45}]_S$

(iv) $[Ø_3 / 6Ø_3 / Ø_3 / \overline{6Ø}]_S$

2.4 PREPARATION OF ENF SPECIMEN

The geometry of ENF specimen size is shown with the starter crack in Fig. 2.6(a). This was cut to the dimensions from a laminate plate (Fig.2.6(b)) with the help of diamond cutter cooled by running water. The sides of the specimen were polished by sand papers of 8Ø and 15Ø grits.

For introducing the starter crack, a thin teflon sheet (Ø.14mm) was placed between 14th and 15th plies for glass fabric reinforced epoxy laminates and between 9th and 1Øth plies in case of carbon fibre reinforced epoxy laminates. It is noted that for this study odd number of plies (29 and 19) were chosen and the crack is not exactly at the mid thickness of the laminate; it is off by only 2.6% of the laminate thickness and can be regarded at the midplane. If even number of plies had been chosen and symmetric laminate was desired, the midplane would have not been an interface. In that case, the precrack would be one ply off (5 2%) from the midplane.

2.5 REINFORCEMENT OF EPOXY RICH INTERFACE WITH ALUMINIUM PARTICLES

The aluminium particles approximately equal to the glass fibre diameter (_ 15μm) were chosen to reinforce the epoxy rich interfaces. To make such laminates the particles were spread on the surfaces of the prepregs through an agitated solution of 2Øgms of aluminium particles in 15Ø ml of acetone. The particles were spread uniformly on one side of the prepreg plies. Acetone vaporized after some time leaving only aluminium particles on the surface. Afterwards, these plies were stacked together and the

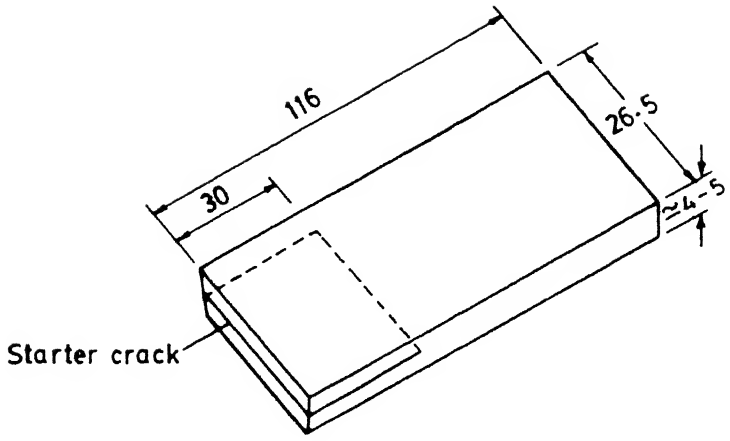

(a)

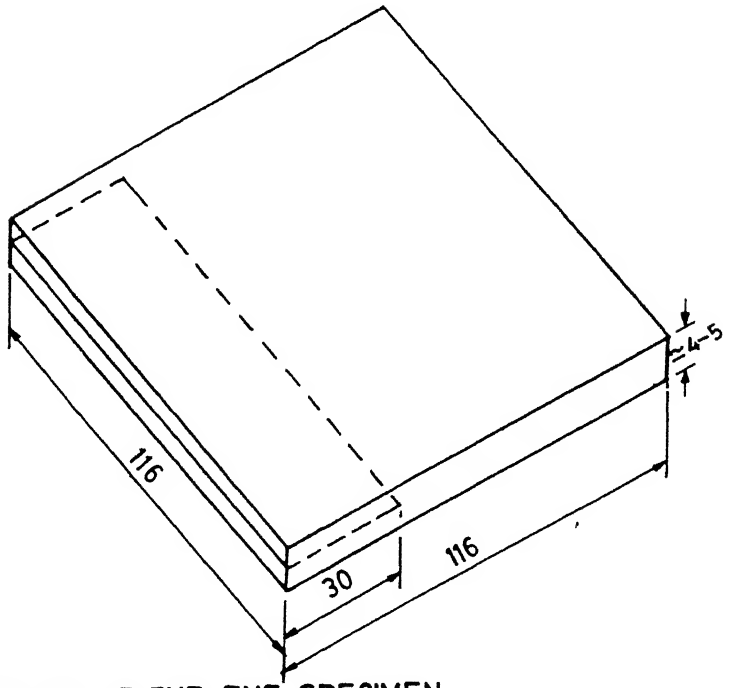

(b)

FIG. 2·6(a) GEOMETRY OF THE ENF SPECIMEN
(b) GEOMETRY OF THE COMPOSITE LAMINATE PROVIDING 4 SPECIMENS

procedure of sec.2.2 and sec.2.3. was followed to obtain the final laminate. Different laminates as in sec.2.2 and 2.3 were prepared. ENF specimen was prepared was done as explained in sec.2.4.

2.6 VOLUME FRACTION OF ALUMINIUM PARTICLES V_{fAl}

The laminates with and without particles spread at the interfaces were weighed independently. The weight fraction of the particles in case of glass & carbon was found to be Ø.6724 Kg/m and Ø.3226 Kg/m respectively. The volume fraction of aluminium particles in the case of glass & carbon was found to be 5.343% and 1.756% respectively.

CHAPTER 3

MODE II INTERLAMINAR FRACTURE TOUGHNESS DETERMINATION

3.1 INTRODUCTION

In this chapter the method for determining the fracture toughness of delamination is explained. The energy release rate G_{II} is chosen as the suitable parameter to characterize interlaminar fracture toughness. End notched fracture ENF specimen is used for the experiment.

3.2 EXPRESSION FOR ENERGY RELEASE RATE 'G'

For a linear elastic body, the relation between the load and displacement may be expressed as

$$u = CP \qquad (3.1)$$

where C is the compliance of the specimen, P is the load applied and u is the displacement.

The energy release rate is given by [12,13,14]

$$G = \frac{P^2}{2}\frac{dC}{dA} \qquad (3.2)$$

where, A is the area of the crack-surface. The above expression is valid for both load control and displacement control experiment.

3.3 END NOTCHED FLEXURE TEST EXPERIMENT

The ENF test is essentially a three point flexure specimen with an starter crack length 'a' placed at the laminate midsurface (Fig. 3.1). The purpose of the test is to determine the critical strain energy release rate in pure mode II loading. From elastic beam theory an expression for strain energy release

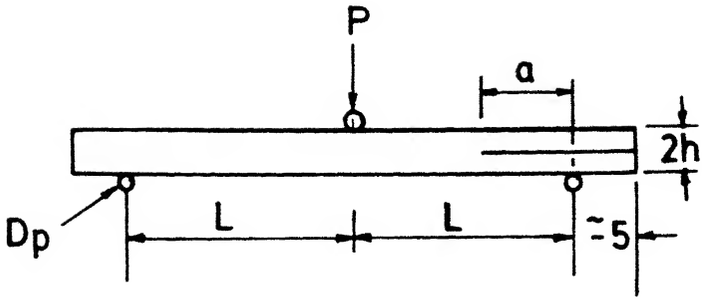

FIG. 3.1 ENF LOADING OF THE SPECIMEN IN MODE II

FIG. 3.2 THREE POINT LOADING OF ENF SPECIMEN BY INSTRON MACHINE

rate can be derived [8,15] as

$$G_{II} = \frac{9\ P^2\ C\ a^2}{2\ w\ [\ 2L^3 + 3a^3\ ]} \qquad (\ 3.3\ )$$

where P is the applied load, C is the compliance, w is the width of the specimen and L is the span between the central loading pin and the outer support pins. For completeness the derivation of the above equation is given in appendix A.

The compliance of the beam may be calculated from the following formula based on beam theory [8,15].

$$C = \frac{2L^3 + 3a^3}{8\ E\ w\ h^3} \qquad (\ 3.4\ )$$

where E is the flexural modulus in the axial direction of the beam and h is the semithickness of the beam. The compliance was determined experimentally rather than using the above formula. In the above derivations deformations due to the action of shear stress and influence of friction between the crack surface were neglected. It is shown in [8], that the specimen has been found to produce shear loading at the crack tip without excessive friction between the crack surfaces.

3.4 STABILITY OF CRACK GROWTH

Stable crack growth required $\frac{dG}{da}$ to be less than or equal to zero.

$$\frac{dG}{da} <= \emptyset$$

For fixed load conditions Eqs.(3.3) and (3.9) gives

$$\frac{dG_{II}}{da} = \frac{9\ a\ P^2}{8\ E\ w^2\ h^3} \qquad (3.5)$$

For the displacement control case of this study, substituting P = u/C (where u is the centre load displacement) in Eq. (3.3) and using Eq. (3.4) we get,

$$\frac{dG_{II}}{da} = \frac{9\ u^2\ a}{8\ E\ w^2\ h^3\ C}\left[\ 1\ -\ \frac{9\ a^3}{(\ 2\ L^3\ +\ 3\ a^3\ )}\ \right] \qquad (3.6)$$

For stable crack growth $\frac{dG_{II}}{da}$ has to be less than or equal to zero. This gives,

$$a\ >\ \frac{L^{\emptyset.33}}{3}\ =\ \emptyset.7\ L$$

Since in the present testing a ≈ Ø.5L the crack growth is unstable even under the displacement control test.

From the load displacement curves of the ENF test, the compliance C and the critical load P for crack propagation are determined and G_{IIc} is computed using Eq.(3.3).

3.5 PRECRACKING OF ENF SPECIMEN

The teflon which was used to produce starter crack was considerably thick (14Ø μm) and at the crack edge the crack may be blunt. As a result the embedded defect may yield artificially high values of mode II fracture toughness [1Ø]. Consequently, prior to fracture test, a precrack was introduced. The method of introducing a precrack is shown in Fig. 3.2*. The total span 2L

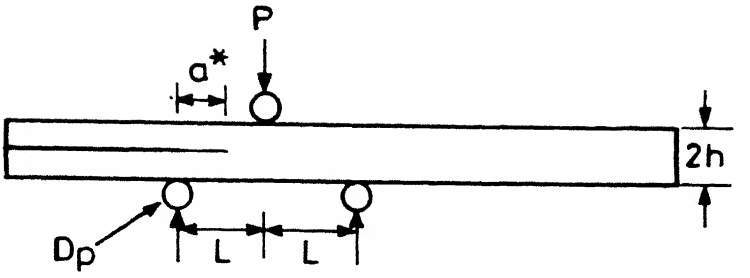

P = LOAD APPLIED
$a^* \simeq 7$ mm
$2h \simeq 3$ to 5mm
L = 12mm
D_p = 9.5mm

Fig. 3.2* PRECRACKING TECHNIQUE FOR ENF SPECIMEN IN MODE II.

= 24 mm was kept and crack length of 7 mm is allowed to grow by application of load at the central loading pin, therefore it is primarily a 3-point bending. The crack grows in an unstable manner till central loading pin. A precrack of approximately 5 mm length was achieved.

3.6 EXPERIMENTAL DETAILS

The specimen was subjected to three point bending on a properly aligned and calibrated Instron machine model 1195. The initial crack length was adjusted to 25 mm in all experiments. The specimen loading test set-up is shown in Fig 3.2. The test was carried on in displacement control. A cross head speed of 2 mm/min was used. The load cell was 1ØØ KN (maximum capacity) and the load range set was 2 KN.

A real time plot of the load versus displacement was made on an X - Y recorder and is shown in Fig. 3.3 for the case of 15° specimen of the glass fabric reinforced epoxy specimen. Since the crack growth was unstable the load drops suddenly.

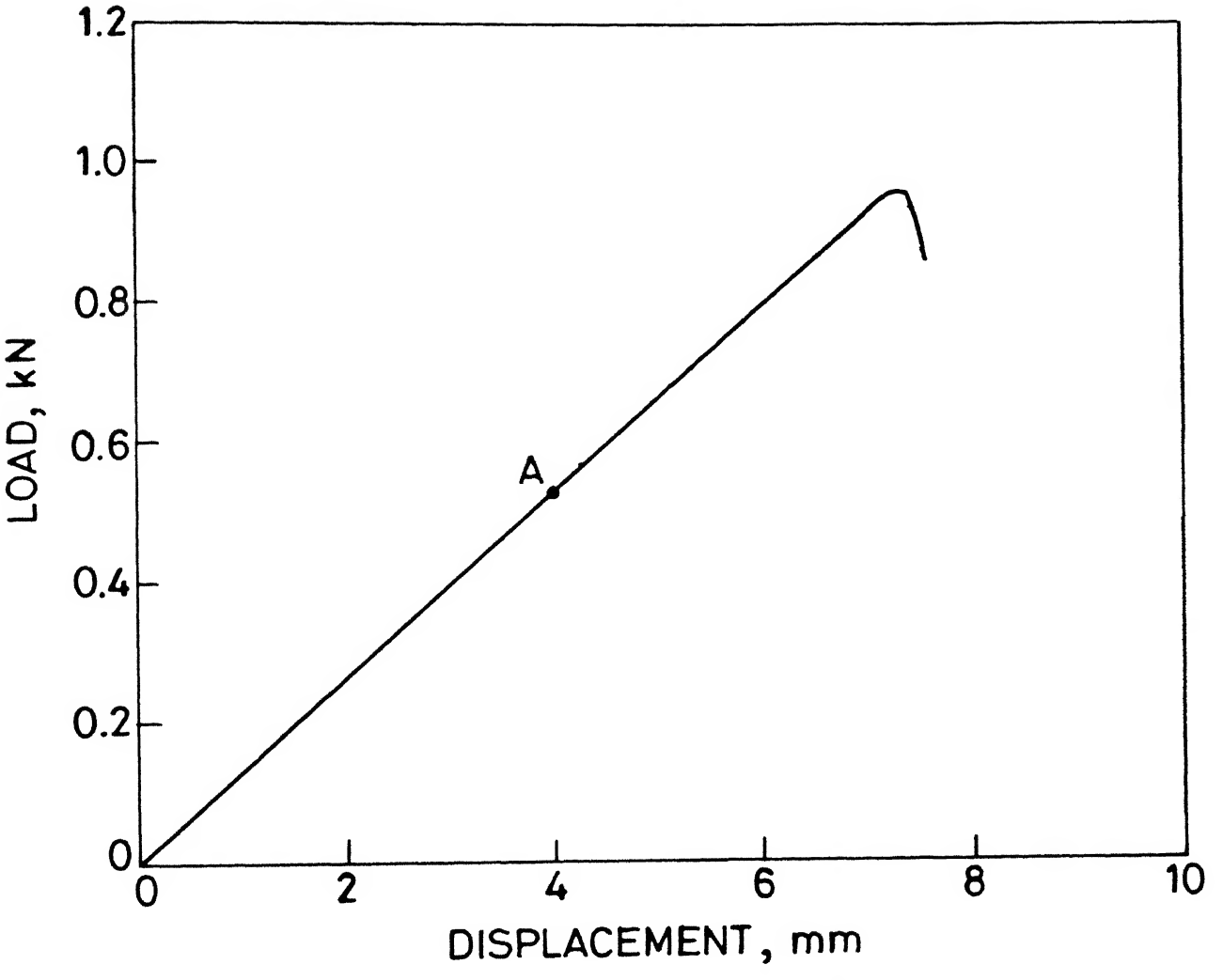

Fig. 3.3 Load deflection curve of ENF test on the Glass Fabric Reinforced Epoxy specimen with ply angle 15°.

CHAPTER 4

RESULTS AND DISCUSSION

4.1 INTRODUCTION

The interlaminar fracture toughness tests were conducted on precracked ENF specimens under mode II made from glass fabric reinforced epoxy prepregs. The tests were also carried out on angle ply laminates made from carbon fibre reinforced epoxy. Micrographs of fractured surfaces of glass fabric reinforced epoxy specimens were studied through a scanning electron microscope.

4.2 MODE II FRACTURE TOUGHNESS FOR GLASS FABRIC REINFORCED EPOXY LAMINATES

As described in sec. 2.2. the specimens for different orientations with and without particles were tested for mode II interlaminar fracture toughness.

The load displacement curve for the precracked specimen of 3-point bending test was obtained as described in sec. 3.6. The load-displacement curve was slightly non-linear in all the cases (Fig. 3.3).

Table 1 gives details of the experiments along with the values of G_{IIc} Fig. 4.1 shows the graph between fracture toughness G_{IIc} versus ply angle θ°, for the both cases of with and without particles.

It is observed that the fracture toughness in Mode II increased by 13.5% for 15° specimen, 22.8% for 3Ø° specimen and 14.5% for 45° specimens with the reinforcement of particles. However, for θ = Ø° there was a decrease by 11% the decrease was not taken seriously because θ = Ø° case is not an interface (the

Table I : Details of Fracture Toughness Tests (G_{II}) of Glass Fabric Reinforced Epoxy Laments.

Width = 26.5 mm
Initial Crack Length = 25 mm

PLY ANGLE	WITHOUT PARTICLES			WITH PARTICLES				PERCENTAGE CHANGE
	t^* (mm)	P_c^+ (N)	G_{IIc} (J/m^2)	t (mm)	Pc (N)	G_{IIc} (J/m^2)	V_{fAl} %	%
Ø°	4.Ø2	1Ø35 1ØØ8 996 1Ø4Ø 1ØØ2	2774.13 2778.78 256Ø.84 2724.52 2557.68	4.48	993 982 1ØØØ 98Ø 1ØØØ	2253.ØØ 2546.2Ø 2391.11 2299.17 2322.5Ø	5.91	-11.Ø2
15°	4.Ø1	88Ø 82Ø 9ØØ	22ØØ.84 2152.72 2154.74	4.54	1Ø4Ø 1Ø25 95Ø	2636.38 2368.61 236Ø.72	5.Ø2	+13.48
3Ø°	4.Ø1	882 82Ø 842	2153.41 2Ø21.91 1999.47	4.48	1ØØ2 935 1Ø1Ø	25Ø5.7Ø 2472.8Ø 26Ø4.81	5.44	+22.82
45°	4.Ø2	936 81Ø 86Ø	2333.66 2373.47 2284.37	4.54	1121 95Ø 94Ø	28Ø7.8Ø 26Ø4.89 2596.72	4.989	+14.56

* Specimen thickness.

\+ Critical load of 3-point bending tests.

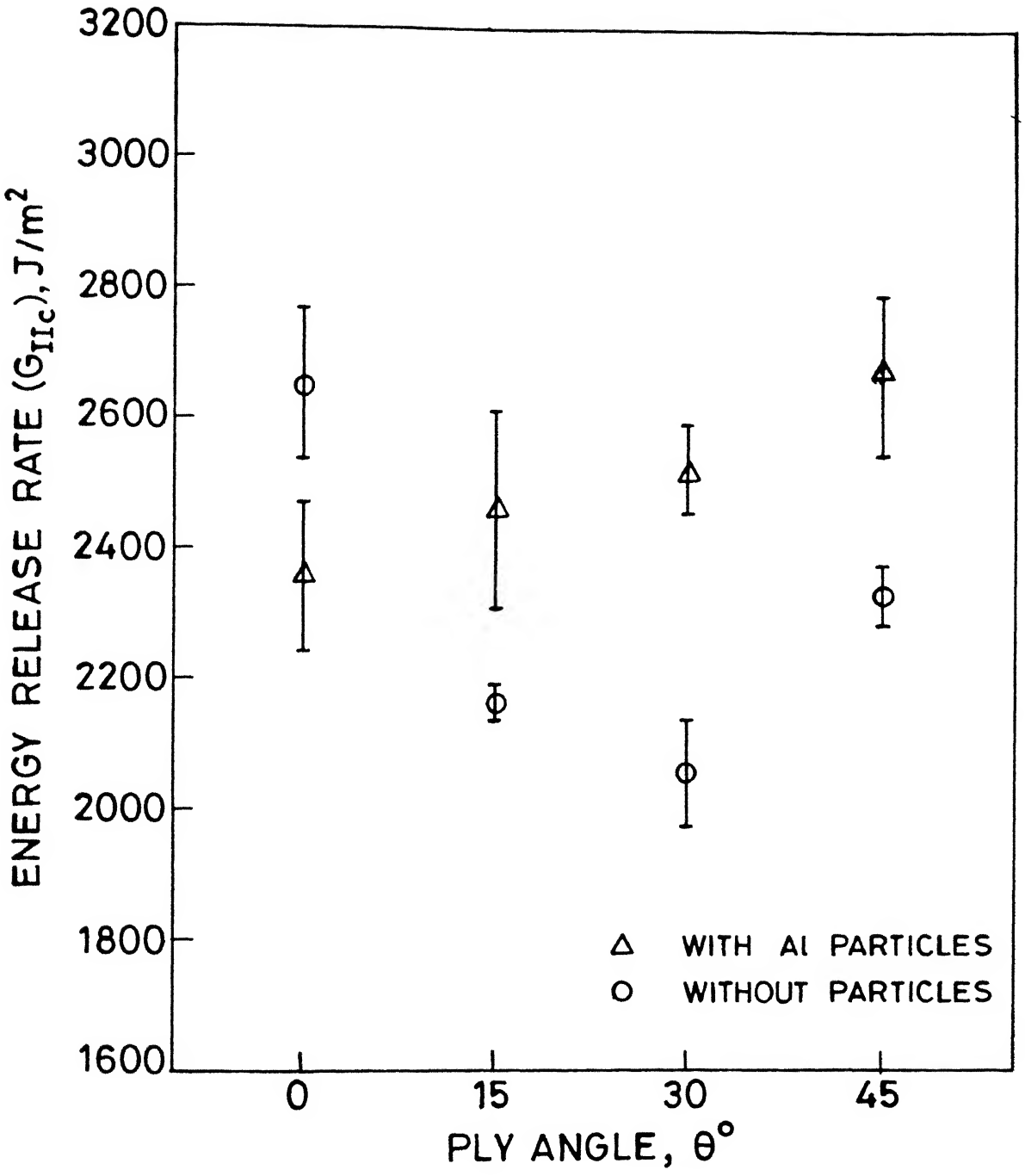

Fig.4.1 Change in energy release rate in mode II (G_{IIc}) of glass fabric reinforced epoxy laminates

stress discontinuity between like plies) and there is no need for particle reinforcement.

With particle reinforcement of the interface, the propagating crack either fractures the relatively more ductile aluminium particle or the cracked plane goes under or over the particles. Micrographs of the fractured surface (discussed subsequently) do not show cracking of the particles. Thus, the actual fracture area increases as the crack goes around the particles. It may be a worthwhile exercise to determine the extent to which the area increases and its effect on fracture toughness.

The largest advantage of particle reinforcement will be in the highly idealized case of particles lying symmetrical with the advancing crack plane ; i.e., the centre of the assumed spheroids are in the plane of the crack. Knowing the weight fraction of the particles and taking average diameter to be equal to 15 μm, the simple calculation would provide an increase of area by 47 %.

Now G_m can be defined on microlevel as,

$$G_m = \frac{\Delta E}{\Delta A} \qquad (4.1)$$

Where, E is the energy required to extend the crack by area A.

$$G = \frac{\Delta E}{\Delta A_{proj.}} \qquad (4.2)$$

Where, $\Delta A_{proj.}$ is the projection of actual fractured area on the cracked plane.

From Eq. 4.1 and Eq. 4.2 we obtain

$$G = \frac{\triangle A}{\triangle A_{proj.}} G_m \qquad (4.3)$$

$$= 1.47\ G_m$$

$$= 47\ \%$$

The possible increase is 47 % under ideal conditions. However, such idealization is far from reality and increase of about 15 % seems reasonable.

The specimens were also tested for tensile strength and tensile modulus. The tensile strength and modulus are listed in Table II tensile strength is plotted in Fig. 4.2, it is observed that tensile strength increases with the ply angle for both kinds of specimens. However, there was decrease in tensile strength with the reinforcement by particles ; 32.1%, for Ø°, 17.9% for 15°, 12.8% for 3Ø° and 16% for 45° specimens. Contribution of particles towards increase in tensile strength was not expected because, particle reinforcement is of much poor quality when compared with fibre reinforcement. The cross sectional area increases and therefore strength reduces. Area of the laminate increases by 13% but reduction of strength was 17% and therefore most of the reduction in strength was because of the change in cross-sectional area. The damaging effect because of the particles was only 4%.

From Fig. 4.3 it is observed that there was decrease in tensile modulus which was of the order of 2Ø%. The tensile modulus also decreased mostly due to the increase in cross-sectional area (13%) and the damaging effect by particles was 7%.

Table II : Change in Tensile Strength and Modulus in Glass Fabric Reinforced Epoxy Laminates.

Width = 14.76 mm
Initial Crack Length = 116 mm

PLY ANGLE	WITHOUT PARTICLES		WITH PARTICLES		PERCENTAGE CHANGE	
	σ_u^*, MPa	$E_1^{\pm}$, GPa	σ_u, MPa	E_1, GPa	σ_u, %	E_1, %
Ø°	342.98Ø	3Ø.7ØØ	232.86Ø	22.326	-32.1Ø	-27.276
15°	382.2Ø1	28.Ø4Ø	281.Ø25	22.2ØØ	-17.85	-2Ø.82Ø
3Ø°	391.Ø26	23.72Ø	3Ø1.Ø26	2Ø.653	-12.84	-12.93Ø
45°	4Ø9.479	22.11Ø	3Ø7.146	19.52Ø	-16.Ø4	-11.71

* Ultimate Tensile Strength

± Tensile Modulus

σ_u - Ultimate tensile strength

E_1 - Tensile modulus

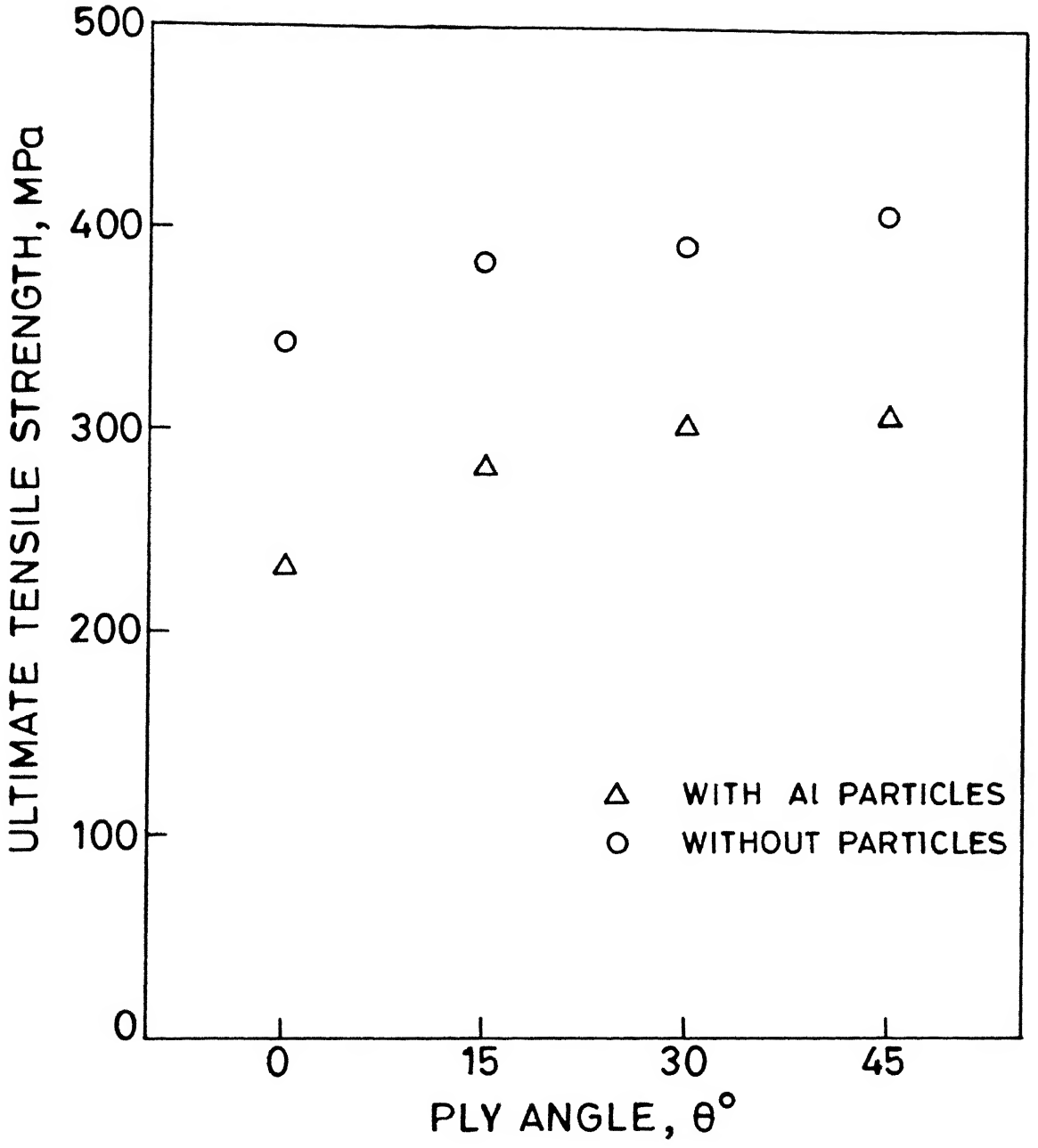

Fig.4.3 Change in tensile modulus of glass fabric reinforced epoxy laminates

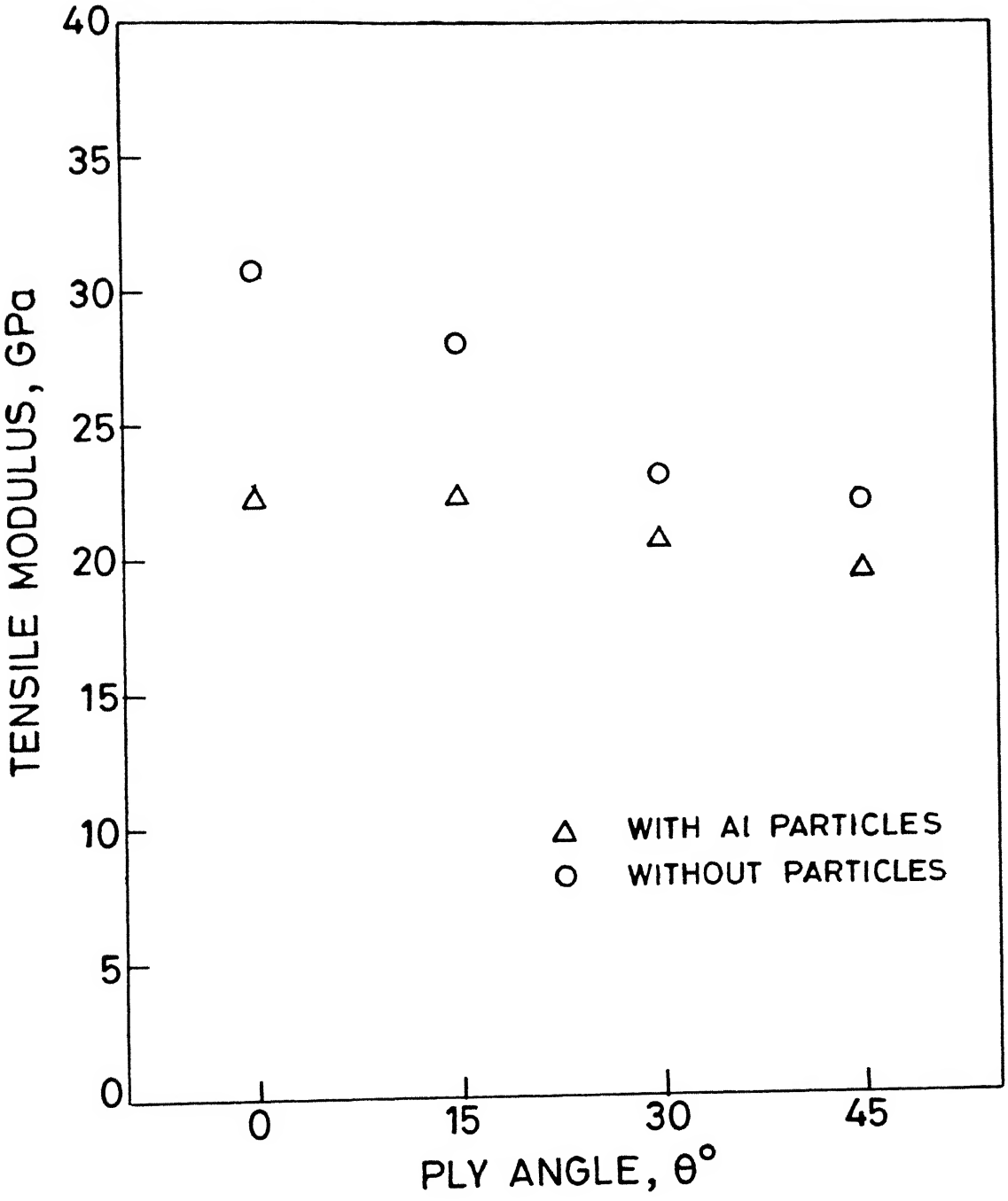

Fig.4.2 Change in ultimate tensile strength of glass fabric reinforced epoxy laminates

4.3 MODE II FRACTURE TOUGHNESS FOR CARBON FIBRE REINFORCED EPOXY LAMINATES

Another set of tests were conducted on angle ply which were different from the glass fabric reinforced epoxy ply; the fibres in the angle ply are straight as against weaved fibres of glass fabric. The specimens for different orientations with and without particles were tested for mode II interlaminar fracture toughness. The load-displacement curve for 3 point bending test on precracked specimen was obtained for each specimen.

Table III gives the G_{IIc} values for 30°, 45°, 60° and 90° specimens. Fig. 4.4 show the graph between fracture toughness G_{II} versus ply angle θ°. Unlike glass fabric reinforced epoxy laminates it is observed that on laminates without particles for θ = 45° shows substantially higher G_{IIc} value over other specimen.

The change in CFRP is mixed, G_{IIc} increased for 30°, 60°, 90° specimens but decreased for 45° specimen. For θ = 30°, 90° the increase in G_{II} was 4% and for θ = 60° the increase was 19%. The decrease in 45° specimen was 24%.

Average increase in fracture toughness G_{IIc} of CFRP laminates with particles was less in comparison to that of glass fabric reinforced epoxy laminates.

The specimens were also tested for tensile strength and tensile modulus. Table IV gives the tensile strength and modulus values. The tensile strength values are plotted in Fig. 4.5. The change in strength was mixed, it increased for 45°, 90°, specimens and decreased for 30°, 60°, specimens. The increase in strength is not understood because increased area of the

Table III: Details of Fracture Toughness Tests (G_{IIc}) of Carbon Fabric Reinforced Epoxy Laminates.

Width = 26.5 mm
Initial Crack Length = 25 mm

PLY ANGLE	WITHOUT PARTICLES			WITH PARTICLES				PERCENTAGE CHANGE
	t^* (mm)	P_c^+ (N)	G_{IIc} (J/m^2)	t (mm)	Pc (N)	G_{IIc} (J/m^2)	V_{fAl} %	%
30°	3.76	903 978 1021 948	828.94 846.68 1036.97 868.69	4.02	1462 1430 1398 1370	924.66 917.49 899.79 1004.11	1.54	+ 4.6
45°	3.79	1460 1578 1560	1578.30 1678.94 1640.27	4.02	1110 1021 1072	1254.03 1252.04 1192.14	1.92	-24.32
60°	3.76	720 750 732	761.75 802.01 784.01	3.92	932 950 1000	864.62 896.72 1032.47	1.68	+18.99
90°	3.66	900 918 1010	851.39 869.80 1066.74	4.01	950 1000 1080	813.24 979.04 1131.70	1.88	+4.88

* Specimen thickness

\+ Critical load of 3-point bending test

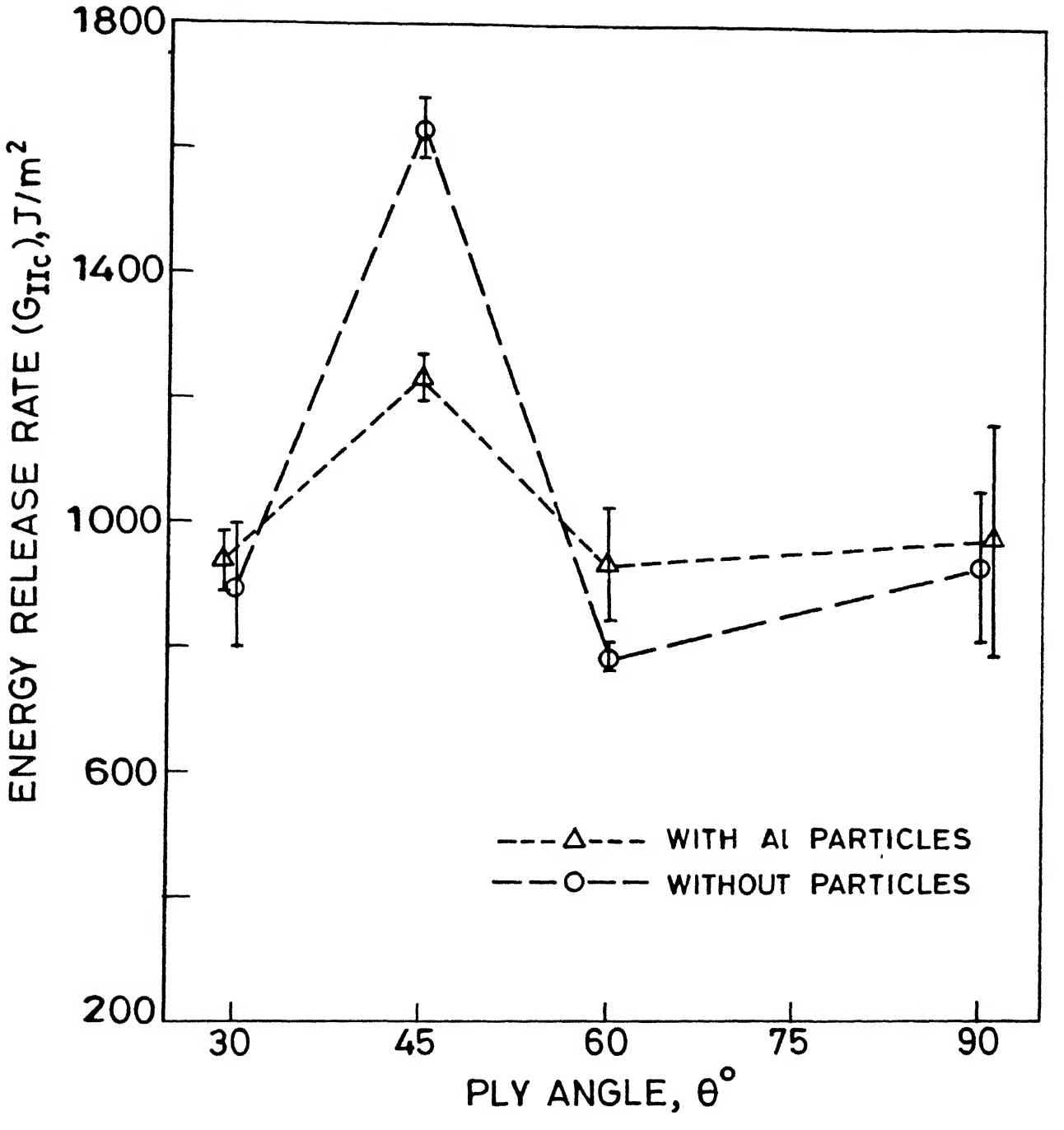

Fig.4.4 Change in energy release rate in mode II (G_{IIc}) of carbon fabric reinforced epoxy laminates

Table IV : Change in Tensile Strength and Modulus in Carbon Fabric Reinforced Epoxy Laminates.

Width = 15 mm
Initial Crack Length= 122 mm

PLY ANGLE	WITHOUT PARTICLES		WITH PARTICLES		PERCENTAGE CHANGE	
	σ_u, MPa	E_1, GPa	σ_u, MPa	E_1, GPa	σ_{ut} %	E_1, %
30°	610.352	98.550	472.169	84.9246	-22.64	-13.82
45°	397.638	61.364	475.084	66.392	+19.47	+18.193
60°	460.250	84.654	427.520	72.463	- 7.11	-14.40
90°	367.077	72.316	429.169	76.446	+16.91	+ 5.69

σ_u - Ultimate tensile strength

E_1 - Tensile modulus

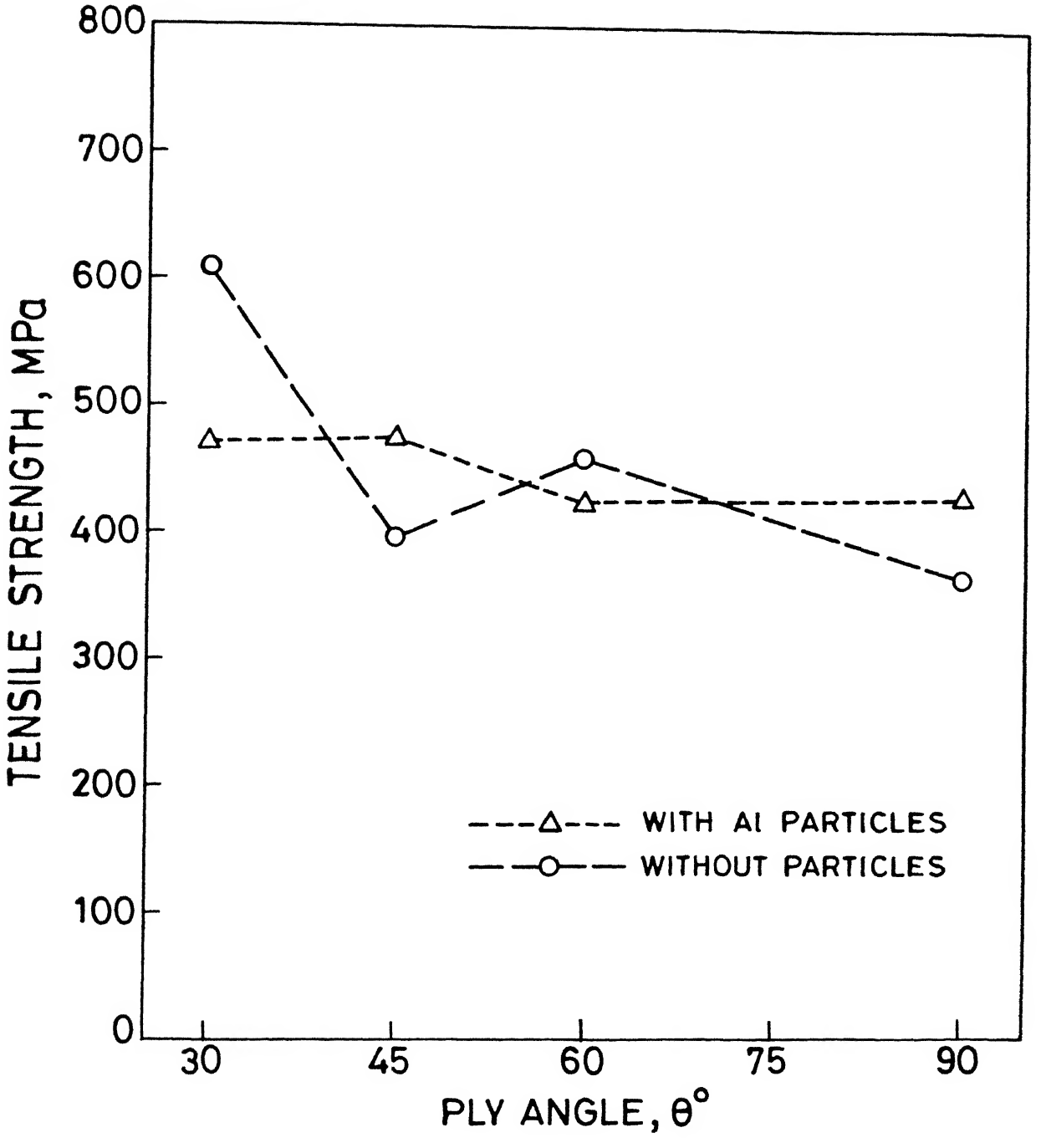

Fig.4.5 Change in ultimate tensile strength of carbon fabric reinforced epoxy laminates

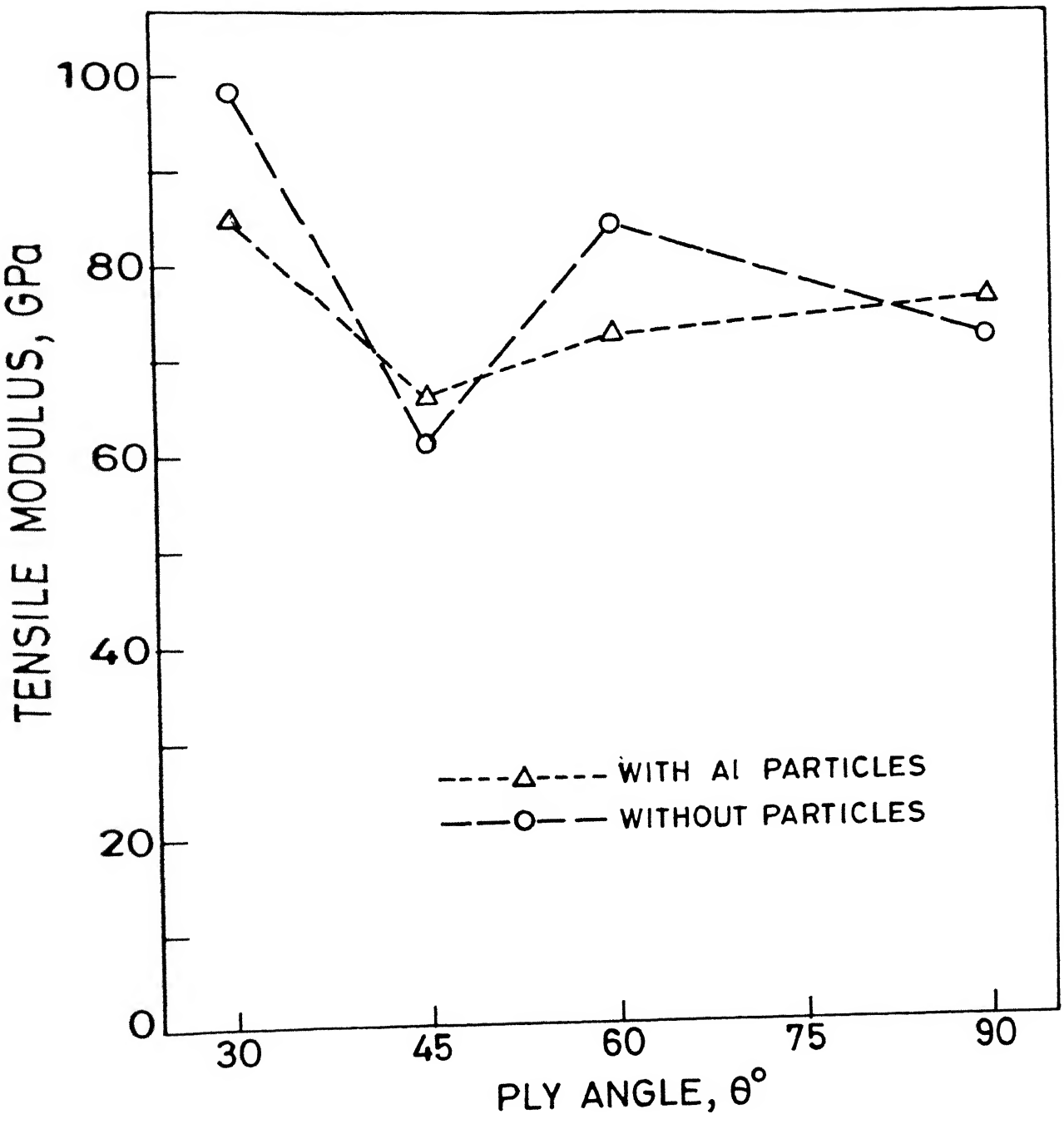

Fig. 4.6 Change in tensile modulus of carbon fibre reinforced epoxy laminates

particle laminate should have decreased the tensile strength.

From Fig. 4.6; it is again observed that the change is mixed. For 3Ø° & 45° there was decrease in tensile modulus by 14% and for 6Ø° & 9Ø° the increase in tensile modulus is also unexplained.

It is observed, that variation in tensile strength and tensile modulus is moderate.

4.4 MICROGRAPH FOR FRACTURED SURFACES OF GLASS FABRIC REINFORCED EPOXY LAMINATES

The micrograph study of the fractured surfaces for glass fabric reinforced epoxy laminates was carried out on scanning electron microscope (SEM).

The specimens were cut to 1Ø mm x 1Ø mm size which were gold plated under vacuum such that the surface becomes conductive. The fractured surfaces were observed under SEM.

Micrographs of the fractured surfaces of Ø° specimen of glass fabric reinforced epoxy laminates are shown in Fig. 4.7a. (without particles) and Fig. 4.7b. (with particles). Fibres are uniformly exposed on the surface of the specimen without particles whereas in particle laminate, fibres bow into the material at several places. This is probably due to the effect of particles which generate high pressure around themselves during the casting. The bowing effect is not desirable because they reduce the stiffness and to certain extent develop stress concentration which in turn decreases the strength.

The bowing in effect of fibres in particle laminates was also observed in 15°, 3Ø°, and 45° specimens as shown in Fig.

4.8(a) and (b). The effect influences the strength and modulus of the particle laminates. For example in 15° specimen, strength reduction was 17% but area correction only accounts for 13%. The difference is most probably due to the bowing in effect. The effect is more pronounced for stiffness as the reduction was 20% out of which only 13% is accounted by the area increase.

At the right hand side of a micrograph, the scale is indicated by a bar. Also, the direction of the advancing crack is shown either by 'I' or a horizontal bar(-).

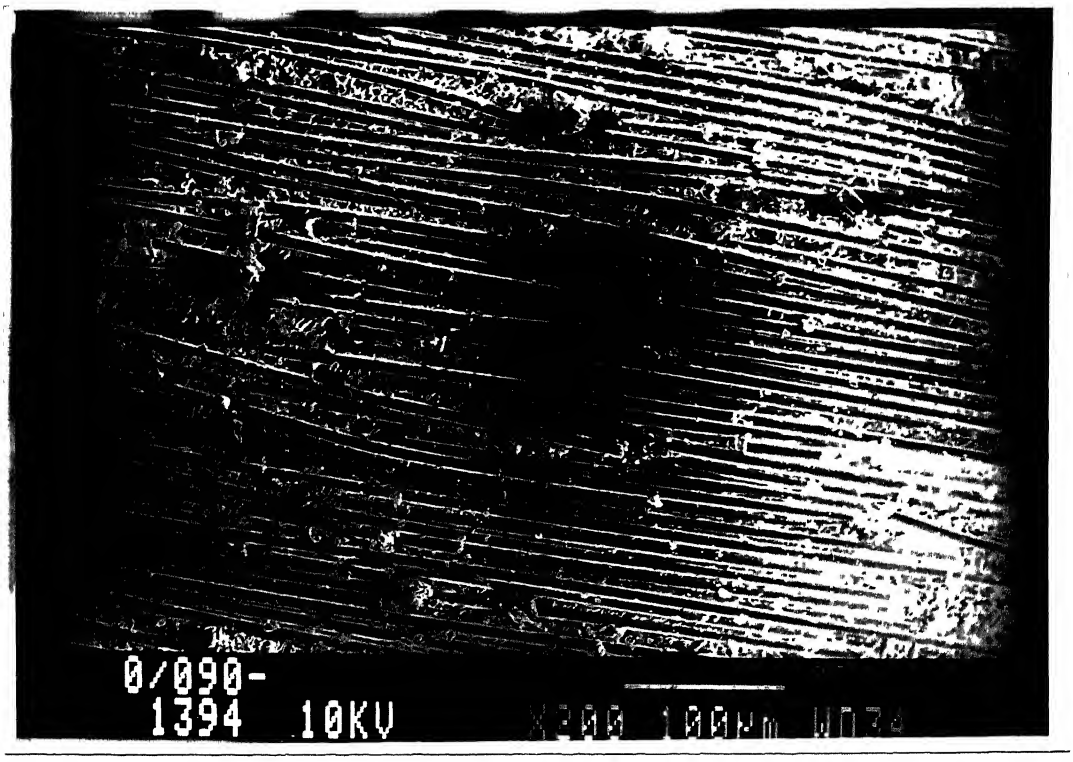

Fig.4.7(a) Fractured surface of [Ø/9Ø] specimen without particles

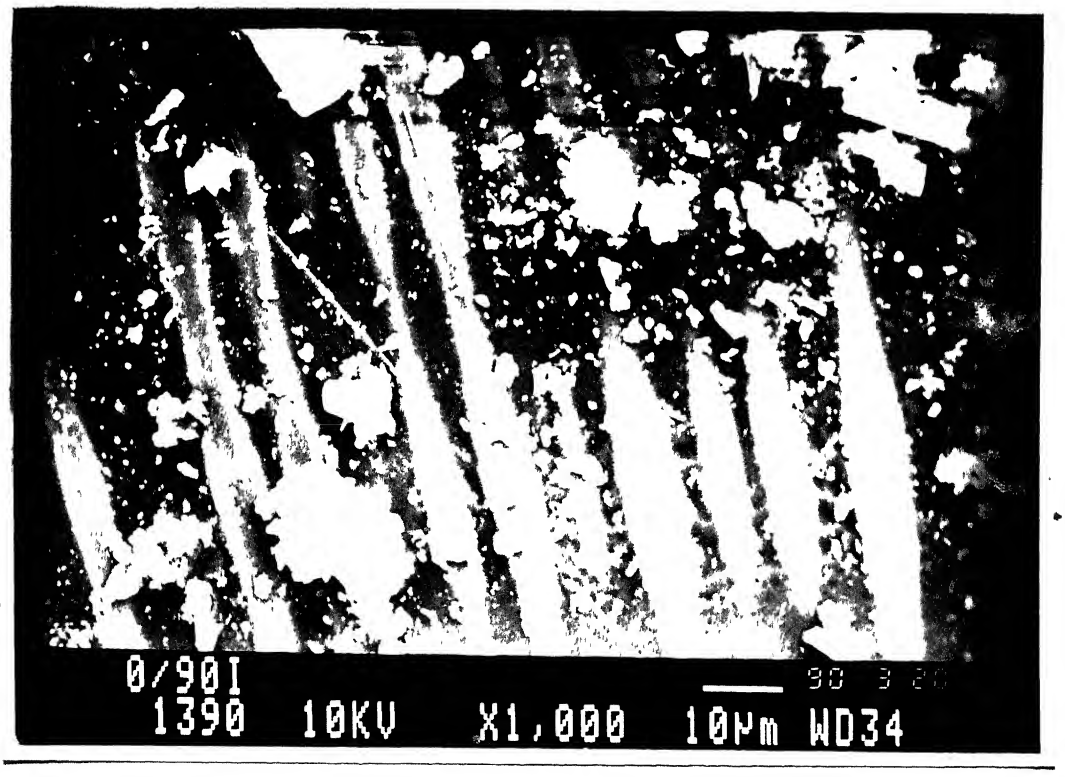

Fig.4.7(b) Fractured surface of [Ø/9Ø] specimen with particles

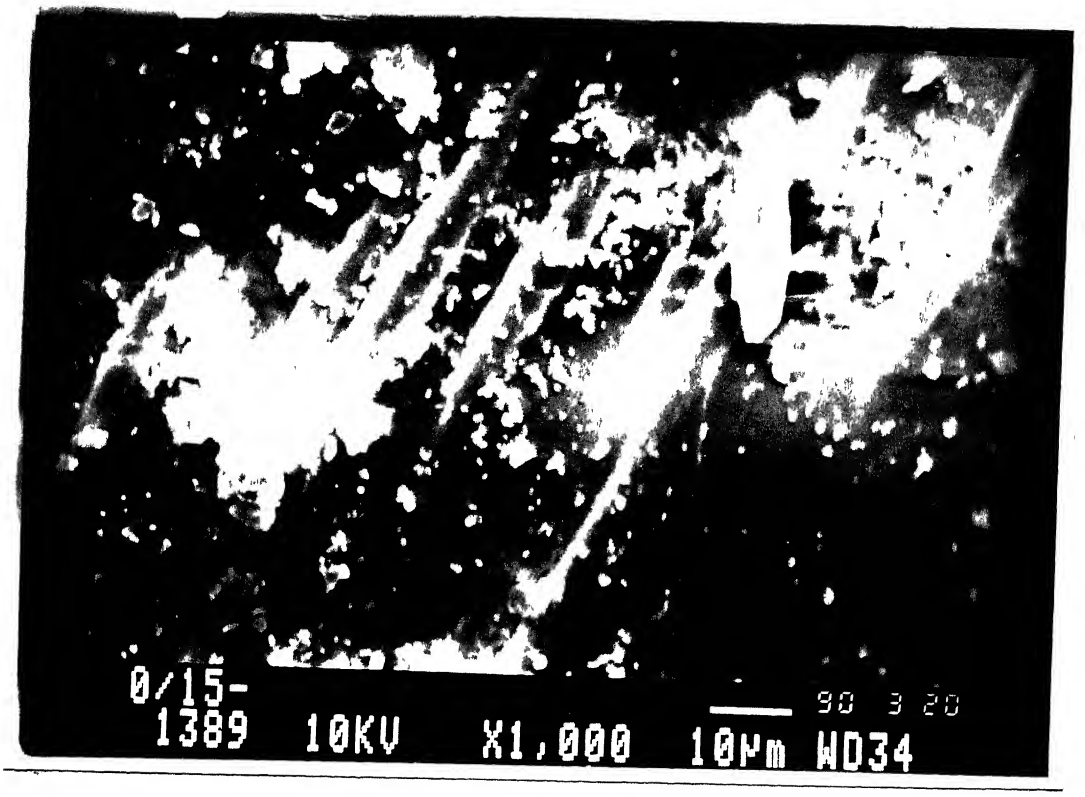

Fig.4.8(a) Fractured surface of [Ø/15] specimen with particles

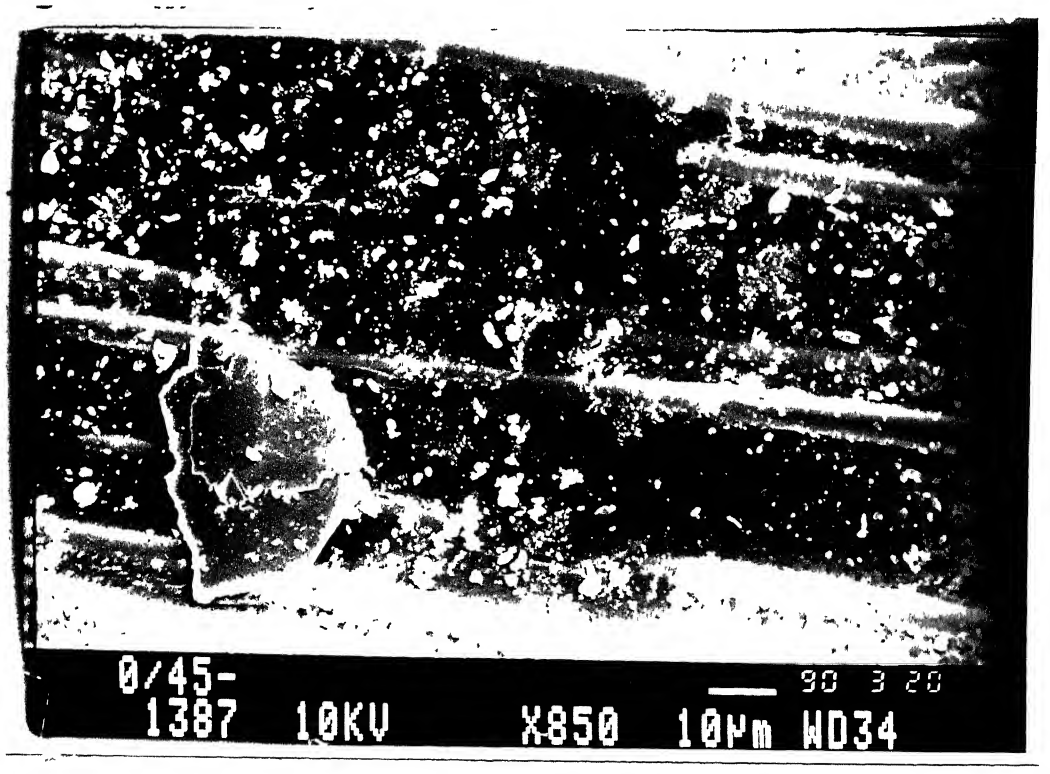

Fig.4.8(b) Fractured surface of [Ø/45] specimen with particles

CHAPTER 5

CONCLUSIONS AND SCOPE FOR FURTHER WORK

Effect of reinforcing the interfaces by aluminium particles was studied on two kinds of laminates of glass fabric reinforced epoxy and carbon fibre reinforced epoxy. The interlaminar fracture toughness values in mode II were determined experimentally using energy release rate approach, by loading precracked ENF specimen on a three point bending feature.

When interfaces of the glass fabric reinforced epoxy laminates were reinforced by aluminium particles the fracture toughness G_{IIc} increased for 15°, 3Ø°, 45° specimen by an average value of 16.5%. However, Ø° specimen, which is really not an interface, showed decrease in G_{IIc}. Average tensile strength was decreased by 18.5%, and tensile modulus decreased by 2Ø%. Effect of particle reinforcement in carbon fibre reinforced epoxy laminates was mixed for fracture toughness G_{IIc}, tensile strength and tensile modulus.

Micrographs of fractured surfaces of the glass fabric-reinforced epoxy laminates showed that the aluminium particles caused the bowing of the fibres.

SCOPE FOR FUTURE WORK

1. More work is required in the case of carbon fibre reinforced epoxy laminates to explain the mixed behaviour which was observed in the present work.

2. More epoxy could be applied at the interfaces of CFRP to ensure complete wetting of the particles.

3. Micrographs study should be carried out further to see the effect of particles.

4. The study can be carried out for different particle sizes preferably with smaller particles which would sit between the fibres better and cause less bowing in effect.

5. If laminates are made from prepregs ; better technique of spraying particles should be developed. It should spray particles more uniformly.

APPENDIX A

EXPRESSION FOR ENERGY RELEASE RATE G_{II}

The derivation of G_{II} is based on the change in compliance with crack extension. The compliance of the ENF specimen is defined as the displacement u at the central loading pin divided by the applied load, P. The expression for G_{II} can be obtained from the work of Carlson et al. [8]. With the notations in the Fig. A.1, u may be calculated as

$$u = \frac{(\Delta_{AB} + \Delta_{BC} + \Delta_{CD})}{2} \qquad (A.1)$$

In the following derivation, deformation due to shear stress is neglected. The beams BC and CD are modelled as cantilever beams with elastic modulus E and thickness 2h. Assuming that the cross section at C does not warp because the line of load is an approximate line of symmetry, the following expressions can be calculated using Timoshenko [15] beam theory.

$$\Delta_{CD} = \frac{P L^3}{4E w h^3} \qquad (A.2)$$

$$\Delta_{BC} = \frac{P (2L^3 + 3aL^2 + a^3)}{8E w h^3} . \qquad (A.3)$$

For the delaminated region AB, the displacement $_{AB}$ has two components. One due to bending of the beams and other due to rotation of the cross section at section B (Figs. A.1 and A.2). Assuming that each beam of the delaminated region carries the same load P/4, the displacement component due to bending may be

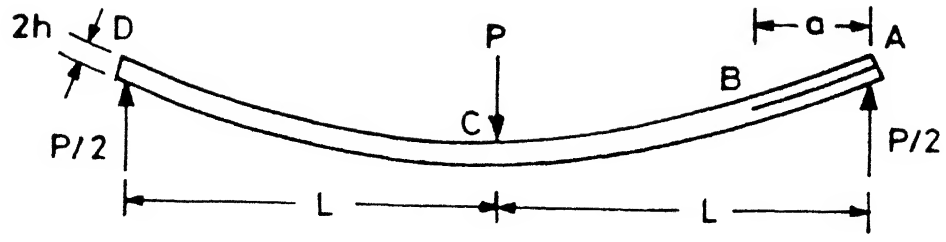

Fig.A1 ENF specimen in bending. Width of the specimen is w.

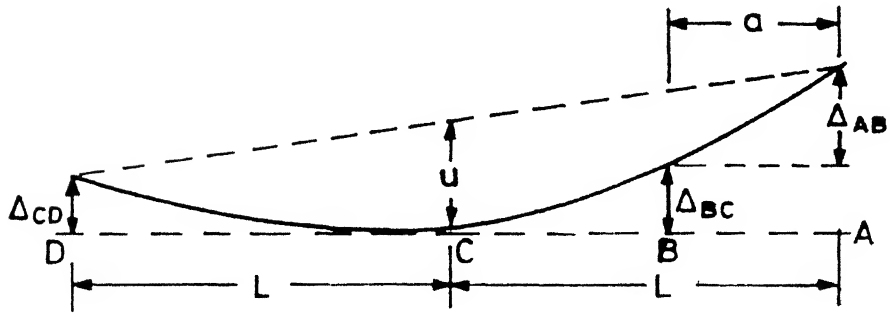

Fig.A2 Definition of vertical displacement for the ENF specimen.

calculated [15] from

$$\Delta_{AB,1} = \frac{P\,a^3}{E\,w\,h^3} \qquad (A.4)$$

The rotation of the cross section at B is expressed as the slope of the cross-section with respect to the horizontal axis. The slope of the cross-section is obtained by summing up the slope produced due to load P/2 and a moment M (= P/2 La) using expressions in [15]. The displacement component due to slope, $\Delta_{AB,2}$ is the slope at B multiplied by the length of the delaminated region. This gives

$$\Delta_{AB,2} = \frac{3P}{8E\,w\,h^3}\,(\,aL^2 - a^3\,) \qquad (A.5)$$

Adding all the contributions to the displacement (eqns. A.2 - A.5) and substituting in eq. (A.1) gives the compliance as,

$$C = \frac{2L^3 + 3a^3}{8E\,w\,h^3} \qquad (A.6)$$

Now using the general expression for energy release rate (eqn 3.9) given in Sec. 3.2, that is,

$$G_{II} = \frac{P^2}{2w}\,\frac{dC}{da}$$

we get,

$$G_{II} = \frac{9\,a^2\,P^2}{16\,E\,w^2\,h^2} \qquad (A.7)$$

Since the compliance is experimentally evaluated, the modulus 'E' in eq (A.7) can be substituted in terms of compliance

'C' using eq. (A.6) to get

$$G_{II} = \frac{9\ P^2\ C\ a^2}{2w\ (\ 2L^3 + 3a^3)} \qquad (A.8)$$

Eq. (A.8) was used in the evaluation of G_{II}.

REFERENCES

[1] B. D. Agarwal and L. J. Broutman, "Analysis and Performance of Fibre Composites", New York, John Wiley, 198Ø.

[2] A. A. Griffith, "The performance of Rupture and Flow in Solids", Phil. Trans. Roy. Soc. of London, A221, 192Ø pp163-197.

[3] G. R. Irwin, "Analysis of Stresses and Strains near the end of a crack traversing a plate", Trans. ASME J. Applied mechanics, Vol. 24, 1957, pp 361-364.

[4] I. Verposest, M. Wevers, P. Meester, "2.5D-Fabrics for delamination resistant Composite Laminates", ICCM VII, Vol.2, 1989, pp 322-328.

[5] A. C. Garg, "Delamination - A life limiting damage mode in aerospace composite structures", Proceedings of the Workshop on Delamination in Composites 19-2Ø March 1987, pp 1Ø4-161.

[6] David W. Baker. US Army Material Commands Service and Technology Centre far East, Fuss-shi, Tokyo.

[7] Russell and K. N. Street, ASTM STP 876(1985), 349.

[8] L. A. Carlsson, J. W. Gillespie, Jr., and R. B. Pipes, "On the Design and Analysis of the End Notched Flexure (ENF) Specimen for Mode II Testing", J. Composite Materials, Vol.2Ø, 1986, pp 594-6Ø4.

[9] T. Vu Khanh, R. Langlois, "On influence of ply orientation of the measurement of Mode II delamination", ICCM Procedings of the 7th International conference on Composite Materials, Vol.2, 1989, pp 633-638.

[1Ø] J. M. Whitney, Hironori Maikuma and J. W. Gillespie, Jr., "On Analysis and Experimental Characterisation of the Centre Notched Flexure Test Specimen for Mode II Interlaminar Fracture", J. Composite Materials, Vol. 2Ø, Aug. 1989, pp756-785.

[11] G. Moron, I. Roman, H. Harel and M. Rosensaft, "The Characterisation of Mode I and Mode II Delamination Failures in Fabric-reinforced Laminates", VI ICCM Vol. 3, 1987, pp 265-273.

[12] Elementary Engineering Fracture Mechanics, David Broek, 1982, Martinus Nijhoff Publishers, Boston.

[13] M. D. Narayanan, "Thesis Entitled Energy Release Rates in Delamination of Glass Fabric, Reinforced Composite Laminates".

[14] S. A. Megeuid, "Engineering Fracture Mechanics", Elsevier Applied Science London and New York.

[15] S. P. Timoshenko and D. H. Young, "Elements of Strength of Materials", East-West Edition 1968.

[16] Jun Xiao and Shun-lin Li, "On Mode II Delamination Fracture Toughness of Multi-directional Interface in Composite Laminate", ICCM Procedings of the 7th International conference on Composite Materials,Vol.2, 1989, pp 669-674.

[17] S. Hashemi, A. J. Kinloch and J. G. Williams, "Interlaminar fracture of the composite materials", 6th ICCM,Vol.3, 1987, pp254-262.